Grid Evolution Based on Cluster Fusion for Doubly Fractional Channel Estimation in OTFS Systems

Xiangjun Li, Qianli Wang, Zilong Liu, Zhengchun Zhou

Abstract—In orthogonal time-frequency space communications, the performance of the uniform grid channel estimation (CE) is generally determined by the delay-Doppler (DD) grid density. A finer grid interval is needed to reduce modeling errors, but this could result in a significantly higher CE complexity when traditional methods are used. Although the grid evolution (GE) method can achieve a good trade-off between complexity and CE performance, there are still many redundant DD grid points that incur additional computational complexity. To address this issue, a new GE method based on cluster fusion for doubly fractional CE is proposed. Simulation results show that our proposed method leads to improved computational efficiency, and achieves a good trade-off between CE performance and complexity.

Index Terms—OTFS, grid evolution, channel estimation, sparse Bayesian learning, fractional delay-Doppler.

I. INTRODUCTION

THE next generation communication systems must support reliable information exchanges in highly dynamic environments, e.g., low-earth-orbit satellites, vehicle-to-everything sytems, unmanned aerial vehicles, etc. In these environments, the legacy orthogonal frequency division multiplexing (OFDM) may become infeasible as its orthogonality could be destroyed by large Doppler. As a solution, orthogonal time-frequency space (OTFS) modulation has emerged in recent years due to its excellent and robust error rate performance in high mobility channels [1]–[3].

Channel estimation (CE) plays an important role in OTFS system design as it has direct impact to the detection performance. A number of OTFS CE schemes have been proposed. An embedded frame structure and a threshold method are proposed in [2] to estimate the channel. In [4], [5], the authors leveraged the sparsity in the delay-Doppler (DD) domain via orthogonal matching pursuit (OMP) and sparse Bayesian learning (SBL) for CE. It is noted that these works assume that the real-life channel response is exactly on the DD grid points. However, this assumption may not be valid in practice due to the fractional delay and Doppler values in real-world transmission. To address this problem, off-grid sparse Bayesian inference (OGSBI) [6] was proposed in [7], leading to one-dimensional (1D) and two-dimensional (2D) off-grid

Xiangjun Li, Qianli Wang and Zhengchun Zhou are with the School of Info Sci & Tech, Southwest Jiaotong University, Chengdu, China. Zilong Liu is with the School of Computer Science and Electronics Engineering, University of Essex, U. K. This work was supported in part by the National Natural Science Foundation of China Under Grant 62350610267. The work of Z. Liu was supported in part by the UK Engineering and Physical Sciences Research Council under Grant EP/Y000986/1 ('SORT') and by the Royal Society under Grants IEC\R3\223079 and IES\R1\241212, and by the British Council under Grant UKIERI-SPARC/01/22. Emails: lxj@my.swjtu.edu.cn; qianli_wang@qq.com; zilong.liu@essex.ac.uk; zzc@swjtu.edu.cn.

CE schemes. The 1D scheme demonstrates a good performance, but with high complexity. In contrast, the 2D scheme strikes a balance between complexity and performance. A 2D off-grid scheme was developed in [8] to eliminate errors caused by interference between delay and Doppler. Yet it still suffers from a high complexity. Inspired by the grid evolution (GE) method in [9], a GE method for doubly fractional CE is proposed [10]. Different from the method in [9], the GE is a 2D method, whereby the fission and adjustment of grid points are performed separately to avoid unnecessary calculations. Compared with the GE scheme in [11], the number of DD grid points in the GE scheme [10] is adjustable and hence it is generic and more flexible. The GE method [10] achieves a trade-off between complexity and performance by evolving the initial uniform grid into a non-uniform locally dense grid. However, there are still many redundant grid points in the locally dense grids, thus leading to unnecessary calculations.

Against the above background, this work investigates grid evolution based on cluster fusion (GE-CF) CE schemes in doubly selective channels for OTFS systems. Specifically, our proposed GE-CF scheme adaptively evolves from an initial uniform coarse grid to a non-uniform coarse grid without a fixed interval. The GE-CF framework contains four processes, i.e., the learning, the fission, the fusion and the adjustment. The learning process estimates the channel response at the grid points. The fission process adds new grid points along the delay or Doppler dimension to form grid point clusters. The fusion process fuses the grid point cluster determined by the cluster selection criterion into an equivalent grid point to more accurately represent the channel response. The adjustment process combines the off-grid parameters into the current grid for decreasing the modeling error. Compared with the GE schemes [10], the proposed GE-CF scheme yields improved trade-off between complexity and CE performance due to smaller number of grid points.

II. SYSTEM MODELS

A. Signal Model

The DD channel response can be expressed as [1]-[3]

$$h(\nu, \tau) = \sum_{n=1}^{P} h_n \delta(\nu - \nu_n) \delta(\tau - \tau_n), \tag{1}$$

where P is the number of paths, h_n , $\tau_n \in (0, \tau_{\max})$ and $\nu_n \in (-\nu_{\max}, \nu_{\max})$ are the channel coefficient, delay, and Doppler of the n-th path, respectively. The symbol duration

1

and bandwidth of OTFS system are NT and $M\Delta f$, respectively. N, M, T and Δf are number of time slots, number of subcarriers, slots duration and subcarrier spacing, respectively.

In this letter, a single pilot x_p with Doppler index k_p' and delay index l_p' in the DD grid is considered. To reduce interference between data and pilot, both the guard interval and the CE region in [7] is used. The sizes of the CE region are $N_{\rm T}=(2k_{\rm max}+1)$ and $M_{\rm T}=(l_{\rm max}+1)$ respectively, where $k_{\rm max}=\nu_{\rm max}NT$ and $l_{\rm max}=\tau_{\rm max}M\Delta f$. According to [2], [3], [7], the OTFS input-output relationship is

$$y_{\text{DD}}[k, l] = x_p \sum_{n=1}^{P} \tilde{h}_n w_{\nu} (k, k'_p, k_{\nu_n}) w_{\tau}^{\text{H}} (l, l'_p, l_{\tau_n}) + z [k, l],$$
(2)

where $y_{\mathrm{DD}}\left[k,l\right]$ is the received signals in the DD domain, $k \in \left\{k'_p - k_{\mathrm{max}}, \cdots, k'_p + k_{\mathrm{max}}\right\},\ l \in \left\{l'_p, \cdots, l'_p + l_{\mathrm{max}}\right\},\ z[k,l] \sim \mathcal{CN}\left(0,\lambda^{-1}\right)$ is the noise and λ^{-1} is the variance, $\tilde{h}_n = h_n e^{-j2\pi\nu_n\tau_n},\ k_{\nu_n} = \nu_n NT,\ l_{\tau_n} = \tau_n M\Delta f,\ w_{\nu}\left(\cdot\right) = w_{\tau}\left(\cdot\right) = \mathcal{F}\left(\cdot\right)$. In [7], [8], $\mathcal{F}\left(\cdot\right)$ is denoted by

$$\mathcal{F}(\eta, \xi, \gamma) = \frac{1}{Q} \left[e^{-j(Q-1)\pi \frac{\eta - \xi - \gamma}{Q}} \frac{\sin(\pi(\eta - \xi - \gamma))}{\sin(\frac{\pi(\eta - \xi - \gamma)}{Q})} \right],$$
(3)

where Q = N for $w_{\nu}(\cdot)$ and Q = M for $w_{\tau}(\cdot)$.

B. Off-Grid Model and GE Model

A finer grid is usually used for sparse representation as that of [7]. In this case, the grid points of the initial uniform DD grid are $\left\{\left\{\bar{k}_{\nu}\right\} \times \left\{\bar{l}_{\tau}\right\}\right\} \in \mathbb{R}^{L_{\nu} \times L_{\tau}}, \ \bar{k}_{\nu} = \left[-k_{\max}, \cdots, k_{\max}\right]^{\mathrm{T}} \in \mathbb{R}^{L_{\nu} \times 1}, \ \bar{l}_{\tau} = \left[-l_{\max}, \cdots, l_{\max}\right]^{\mathrm{T}} \in \mathbb{R}^{L_{\tau} \times 1}.$ Therefore, the initial delay and Doppler resolution are $r_{\nu} = \frac{2k_{\max}}{L_{\nu}-1}$ and $r_{\tau} = \frac{l_{\max}}{L_{\tau}-1}$, respectively. Let the number of grid points in the sampled DD grid be $L = L_{\nu}L_{\tau}$. After vectorizing the DD grid, all DD grid points can be expressed as $\tilde{S} = \left\{\tilde{k}_{\nu}, \tilde{l}_{\tau}\right\}, \ \tilde{l}_{\tau} = \left[l_{0}, l_{1}, \cdots l_{i}, \cdots, l_{L-1}\right]^{\mathrm{T}}, \ \tilde{k}_{\nu} = \left[k_{0}, k_{1}, \cdots, k_{i}, \cdots, k_{L-1}\right]^{\mathrm{T}}$. Let $i \in \{1, \cdots L\}, \ w_{\nu}(k_{i}) = \left[w_{\nu}\left(k_{p}' - k_{\max}, k_{p}', k_{i}\right), \cdots, w_{\nu}\left(k_{p}' + k_{\max}, k_{p}', k_{i}\right)\right]^{\mathrm{T}} \in \mathbb{C}^{N_{\mathrm{T}} \times 1}, \ w_{\tau}(l_{i}) = \left[w_{\nu}\left(l_{p}', l_{p}', l_{i}\right), \cdots, w_{\nu}\left(l_{p}' + l_{\max}, l_{p}', l_{i}\right)\right]^{\mathrm{T}} \in \mathbb{C}^{M_{\mathrm{T}} \times 1}$. Then, the on-grid model based on Eq. (2) is

$$y = x_p \Phi_{\rm I} \left(\tilde{\mathbf{S}} \right) \tilde{\mathbf{h}} + \mathbf{z},$$
 (4)

where $\boldsymbol{y}, \boldsymbol{z} \in \mathbb{C}^{N_{\mathrm{T}}M_{\mathrm{T}} \times 1}, \ \boldsymbol{y} = \mathrm{vec}\left(\boldsymbol{Y}\right), \ \boldsymbol{Y} \in \mathbb{C}^{N_{\mathrm{T}} \times M_{\mathrm{T}}}$ is the matrix form of $y_{DD}\left[k,l\right], \ \tilde{\boldsymbol{h}} \in \mathbb{C}^{L \times 1}, \ \boldsymbol{\varPhi}_{\mathrm{I}}\left(\tilde{\boldsymbol{S}}\right) = \boldsymbol{\psi} \odot \left[\boldsymbol{\phi}_{\mathrm{I}}\left(k_{0},l_{0}\right), \cdots, \boldsymbol{\phi}_{\mathrm{I}}\left(k_{L-1},l_{L-1}\right)\right] \in \mathbb{C}^{N_{\mathrm{T}}M_{\mathrm{T}} \times L}$ is the on-grid part of the measurement matrix corresponding to the current DD grid, $\boldsymbol{\phi}_{\mathrm{I}}\left(k_{i},l_{i}\right) = \mathrm{vec}\left(\boldsymbol{w}_{\nu}\left(k_{i}\right)\boldsymbol{w}_{\tau}^{H}\left(l_{i}\right)\right) \in \mathbb{C}^{N_{\mathrm{T}}M_{\mathrm{T}} \times 1},$ $\boldsymbol{\psi} = \begin{bmatrix} \boldsymbol{\varphi}_{0}, \cdots, \boldsymbol{\varphi}_{L-1} \end{bmatrix} \in \mathbb{C}^{N_{\mathrm{T}}M_{\mathrm{T}} \times L}, \ \boldsymbol{\varphi}_{i} = e^{\frac{-j2\pi k_{i}l_{i}}{NM}} \mathbf{1}, \mathbf{1} \in \mathbb{C}^{N_{\mathrm{T}}M_{\mathrm{T}} \times 1}$ is the all-ones column vector, $\mathrm{vec}\left(\cdot\right)$ is the vectorization operation, \odot is the dot product.

Since in practice the channel response generally does not fall exactly on the sampled DD grid points, an off-grid CE scheme was proposed in [7], [8]. Denote by $\left(k_i \in \tilde{\boldsymbol{k}}_{\nu}, l_i \in \tilde{\boldsymbol{l}}_{\tau}\right)$ the i-th grid point which is closest to (k_{ν_n}, l_{τ_n}) in the discrete

DD plane. Then a linear approximation in [7] can be obtained by first-order Taylor expansion, i.e,

$$\boldsymbol{\Phi}\left(k_{\nu_{n}}, l_{\tau_{n}}\right) = \boldsymbol{\phi}_{\mathrm{I}}\left(k_{i}, l_{i}\right) + \boldsymbol{\phi}_{\nu}\left(k_{i}, l_{i}\right) \kappa_{i} + \boldsymbol{\phi}_{\tau}\left(k_{i}, l_{i}\right) \iota_{i} + o\left(\kappa_{i}\right) + o\left(\iota_{i}\right),$$
(5)

where $\kappa_i = k_{\nu_n} - k_i$, $\iota_i = l_{\tau_n} - l_i$, $o(\kappa_i)$ and $o(\iota_i)$ are Doppler and delay modeling errors, respectively, $\phi_{\nu}(k_i, l_i) = \text{vec}\left(\boldsymbol{w}_{\nu}'(k_i)\,\boldsymbol{w}_{\tau}^{\text{H}}(l_i)\right)$, $\phi_{\tau}(k_i, l_i) = \text{vec}\left(\boldsymbol{w}_{\nu}(k_i)\,(\boldsymbol{w}_{\tau}'(l_i))^{\text{H}}\right)$, $\boldsymbol{w}_{\nu}'(k_i)$ and $\boldsymbol{w}_{\tau}'(l_i)$ are the partial derivatives with respect to k_i and l_i respectively. Here, κ_i and ι_i are assumed to follow uniform distributions

$$\kappa_i \sim \mathcal{U}\left[-\frac{1}{2}\tilde{r}_{\nu_-}, \frac{1}{2}\tilde{r}_{\nu_+}\right], \iota_i \sim \mathcal{U}\left[-\frac{1}{2}\tilde{r}_{\tau_-}, \frac{1}{2}\tilde{r}_{\tau_+}\right], \quad (6)$$

where \tilde{r}_{ν} and \tilde{r}_{τ} respectively represent the Doppler and delay resolutions between a grid point and its adjacent grid points, + and - denote positive and negative directions respectively. Let $\tilde{\kappa} = \left[\kappa_0, \kappa_1, \cdots, \kappa_{L-1}\right]^{\mathrm{T}} \in \mathbb{C}^{L \times 1}$, $\tilde{\iota} = \left[\iota_0, \iota_1, \cdots, \iota_{L-1}\right]^{\mathrm{T}} \in \mathbb{C}^{L \times 1}$. Similar to $\Phi_{\mathrm{I}}\left(\tilde{\boldsymbol{S}}\right)$, $\phi_{\nu}\left(k_i, l_i\right)$ and $\phi_{\tau}\left(k_i, l_i\right)$ can be arranged in order to obtain $\Phi_{\nu}\left(\tilde{\boldsymbol{S}}\right)$ and $\Phi_{\tau}\left(\tilde{\boldsymbol{S}}\right)$, respectively. Then the measurement matrix $\Phi\left(\tilde{\boldsymbol{S}}, \tilde{\boldsymbol{\kappa}}, \tilde{\boldsymbol{\iota}}\right) \in \mathbb{C}^{N_{\mathrm{T}} M_{\mathrm{T}} \times L}$ can be expressed as

$$\boldsymbol{\Phi}\left(\tilde{\boldsymbol{S}}, \tilde{\boldsymbol{\kappa}}, \tilde{\boldsymbol{\iota}}\right) = \boldsymbol{\Phi}_{\mathrm{I}}\left(\tilde{\boldsymbol{S}}\right) + \boldsymbol{\Phi}_{\nu}\left(\tilde{\boldsymbol{S}}\right) \operatorname{diag}\left\{\tilde{\boldsymbol{\kappa}}\right\} + \boldsymbol{\Phi}_{\tau}\left(\tilde{\boldsymbol{S}}\right) \operatorname{diag}\left\{\tilde{\boldsymbol{\iota}}\right\},$$
(7)

where $\mathrm{diag}\left\{\cdot\right\}$ is the diagonal matrix operator. After absorbing the approximation error into the noise, the observation model can be written as

$$\boldsymbol{y} = x_p \boldsymbol{\Phi} \left(\tilde{\boldsymbol{S}}, \tilde{\boldsymbol{\kappa}}, \tilde{\boldsymbol{\iota}} \right) \tilde{\boldsymbol{h}} + \boldsymbol{z}. \tag{8}$$

Note that \tilde{S} is constant in both the on-grid and off-grid models, meaning that r_{ν} and r_{τ} are constants. As mentioned before, the performance of the on-grid and off-grid models will deteriorate when multiple real-life channel responses are located in the same DD interval. Therefore, the proposed GE scheme uses a varying S to decrease the modeling error, where $S = \left\{ \tilde{S}_{\rm ini}, \tilde{S}_{\rm GE} \right\}$, the $\tilde{S}_{\rm ini}$ is the S with $r_{\nu} = r_{\tau} = 1$, $\tilde{S}_{\rm GE}$ represents the added grid points in the GE scheme. Therefore, the model in GE is,

$$y = x_n \Phi(S, \kappa, \iota) h + z, \tag{9}$$

where the sizes of κ , ι and h are corresponding to S.

III. GRID EVOLUTION BASED ON CLUSTER FUSION CHANNEL ESTIMATION

To get the grid points S and estimate h in Eq. (9), GE method is adopted to increase the local resolution for a more accurate representation of the sparse channel responses in the DD domain. After the fission process, grid point clusters will be generated around the true responses by decreasing the off-grid gaps to distinguish the close paths. A grid point cluster can sparsely represent a true channel response. Ideally, a grid point is sufficient to represent the channel response of a path. Therefore, there are many redundant grid points in the

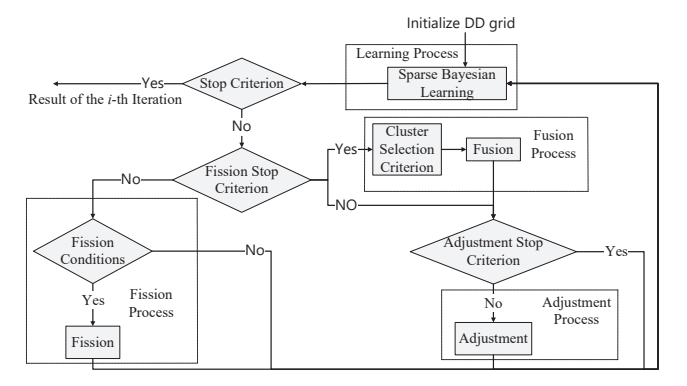


Fig. 1: The procedure of GE channel estimation.

grid point cluster. To avoid unnecessary computational load, a more accurate grid point is needed to replace the grid point cluster. Therefore, in the GE-CF scheme, an appropriate fusion algorithm is employed to fuse the grid point cluster into a new equivalent grid point.

The GE-CF method consists of the learning, the fission, the fusion and the adjustment processes, as shown in Fig. 1. The fission process can distinguish multiple channel responses within the same initial DD interval. The fusion process fuses a grid point cluster into an equivalent grid point to more accurately represent the channel response. The adjustment process combines the off-grid parameters into the current grid to reduce the off-grid gap. The learning process estimates the channel response at the grid points by SBL. These processes are performed sequentially to reduce modeling errors. To strike a trade-off between modeling error and computational workload, stop criteria are proposed for fission and adjustment.

A. Learning Process

OGSBI in [6] is used to estimate the channel parameters in the learning process. According to [6], [7], the posterior conditional distribution of h is assumed to be

$$p(\mathbf{h}|\mathbf{y};\boldsymbol{\alpha},\boldsymbol{\kappa},\boldsymbol{\iota},\lambda) = \mathcal{CN}(\mathbf{h}|\boldsymbol{\mu},\boldsymbol{\Sigma}), \tag{10}$$

where α is the hyperparameter that models the sparsity of h and follows a Gamma distribution controlled by the parameter ρ , λ follows a Gamma distribution determined by a and b, The mean μ and covariance Σ for the (t)-th iteration are

$$\boldsymbol{\mu}^{(t)} = \lambda^{(t)} \boldsymbol{\Sigma}^{(t)} \boldsymbol{\Phi}^{\mathrm{H}} \left(\boldsymbol{S}^{(t)}, \boldsymbol{\kappa}^{(t)}, \boldsymbol{\iota}^{(t)} \right) \boldsymbol{y}, \tag{11}$$

$$\Sigma^{(t)} = \operatorname{diag}\left(\boldsymbol{\alpha}^{(t)}\right) - \left(\boldsymbol{\alpha}^{(t)} \odot \left(\boldsymbol{\alpha}^{(t)} \odot \boldsymbol{C}\right)^{\mathrm{T}}\right)^{\mathrm{T}}, \quad (12)$$

where
$$C = \Phi^{\mathrm{H}}\left(S^{(t)}, \kappa^{(t)}, \iota^{(t)}\right) \Sigma_{\mathrm{y}}^{-1} \Phi\left(S^{(t)}, \kappa^{(t)}, \iota^{(t)}\right),$$

$$\Sigma_{\mathrm{y}} = \Phi\left(S^{(t)}, \kappa^{(t)}, \iota^{(t)}\right) \left(\alpha^{(t)} \odot \Phi^{\mathrm{H}}\left(S^{(t)}, \kappa^{(t)}, \iota^{(t)}\right)\right) + \lambda^{(t)} I, \alpha \odot C$$
 is the dot product of the elements of the column vector α with the corresponding rows of C . Different from the traditional update formulation of Σ , the diagonal matrix property is considered here to reduce the complexity.

The expectation–maximization algorithm is used to update each hyper-parameter for the (t + 1)-th iteration, i.e.,

$$\alpha(i)^{(t+1)} = \frac{\sqrt{1 + 4\rho \left(\Sigma(i,i)^{(t)} + \left|\mu(i)^{(t)}\right|^2\right)} - 1}{2\rho}, \quad (13)$$

$$\lambda^{(t+1)} = \frac{2a - 2 + M_{\rm T} N_{\rm T}}{2b + \Delta u},\tag{14}$$

where $i \in \{1,\cdots,L\}$, $\Delta y = \left(\lambda^{(t)}\right)^{-1} \sum_{i=1}^L 1 - \frac{\Sigma(i,i)^{(t)}}{\alpha(i)^{(t)}} + \left\| \boldsymbol{y} - \boldsymbol{\Phi}\left(\boldsymbol{S}^{(t)}, \boldsymbol{\kappa}^{(t)}, \boldsymbol{\iota}^{(t)}\right) \boldsymbol{\mu}^{(t)} \right\|^2$, $\lambda > 0$, a > 0, b > 0. For updates of off-grid parameters, please refer to [6], [7]. The iteration will stop if $\frac{\left\|\boldsymbol{\alpha}^{(t+1)} - \boldsymbol{\alpha}^{(t)}\right\|}{\left\|\boldsymbol{\alpha}^{(t)}\right\|} < \delta$ or the maximum number of iterations K is reached, where δ is a tolerance.

B. Fission Process

Three fission conditions are used like that of [9], [10] to decide whether a fission of a grid should happen. When these three conditions are met, the fission needs to be carried out simultaneously in both the delay and the Doppler dimensions based on estimated off-grid parameters. Assume that the chosen grid point χ is (k_i, l_i) , $i \in \{1, \cdots, L\}$, and the estimation result of corresponding off-grid parameter is $(\hat{\kappa}_i, \hat{\iota}_i)$. The off-grid parameters can indicate that the channel response is in a certain direction of grid point χ . Thus two new grid points $\chi_k = (k_{\rm fission}, l_i)$ and $\chi_l = (k_i, l_{\rm fission})$ will be generated after fission, where $k_{\rm fission}$ and $l_{\rm fission}$ are

$$k_{\text{fission}} = \begin{cases} k_i + \frac{1}{2}\tilde{r}_{\nu_+}, \hat{\kappa}_i > 0\\ k_i - \frac{1}{2}\tilde{r}_{\nu_-}, \hat{\kappa}_i < 0 \end{cases},$$
(15)

$$l_{\text{fission}} = \begin{cases} l_i + \frac{1}{2}\tilde{r}_{\tau_+}, \hat{\iota}_i > 0 \\ l_i - \frac{1}{2}\tilde{r}_{\tau_-}, \hat{\iota}_i < 0 \end{cases}$$
 (16)

If a grid point fissions, it will be necessary to add 1 or 2 elements corresponding to the grid point for κ , ι and h in Eq. (9). Owing to the OGSBI method we used for estimation, the fission of prior of h, i.e., α , is needed. Assume that the α value corresponding to grid points χ , χ_f , χ_k and χ_l are α_{χ} , α_{χ_f} , α_{χ_k} and α_{χ_l} , respectively, where χ_f is the grid point χ version after fission. To keep the prior $p(\alpha)$ unchanged after fission, $p(\alpha)$ should be a constant [9]. Therefore,

$$\alpha_{\chi_{\rm f}} = \alpha_{\chi_k} = \alpha_{\chi_l} = \frac{1}{3}\alpha_{\chi},\tag{17}$$

where α_{γ} is estimated by Eq. (13).

In addition, the fission stop criterion is introduced that no more fission will happen if the maximum number of iterations $K_{\rm f}$ for fission process is reached. $K_{\rm f}$ may be larger than $\log_2(1/r_{\rm min})$, which refers to the average iteration number for reaching a satisfying resolution.

C. Fusion Process

After the fission process, the fusion process needs to find an equivalent grid point of the grid point cluster. Fusing different clusters generally results in different equivalent grid points, leading to varying CE performance. Such differences are manifested in the positions of the equivalent grid points on the DD grid, as well as in the corresponding hyperparameter α . Therefore, based on the grid point (k_i, l_i) with $|\mu\left(i\right)| > \varepsilon\sqrt{\lambda^{-1}}$, the proposed cluster selection criterion is given by

$$\mathcal{Z} = \{ (k_j, l_j) | |k_j - k_i| \le d, |l_j - l_i| \le d \}, \qquad (18)$$

where $(k_j, l_j) \in S$, $j \in \{1, \cdots, L\}$, S denotes the set of existing grid points, ε is a weight related to miss detection or false-alarm probabilities, $d \geqslant r_{\min}$ is a parameter related to the size of the DD dimension of the cluster. This criterion determines a cluster by d. If d is larger, there will be more grid points in the cluster. However, this may include grid points from another cluster. Therefore, it is necessary to set a suitable d.

After a cluster is determined, the cluster is fused into an equivalent grid point through a fusion algorithm. Assume that the G grid points in a selected cluster are $\{\mathcal{X}_1,\cdots,\mathcal{X}_G\}$, with corresponding DD indices, mean, and hyperparameter α represented by $\{(k_{\mathcal{X}_1},l_{\mathcal{X}_1}),\cdots,(k_{\mathcal{X}_G},l_{\mathcal{X}_G})\}$, $\{\mu_1,\cdots,\mu_G\}$, and $\{\alpha_1,\cdots,\alpha_G\}$, respectively. The simplest fusion method is average fusion (AF), i.e,

$$k_{\rm AF} = \frac{\sum_{g=1}^{G} k_{\mathcal{X}_g}}{G},\tag{19}$$

$$l_{\rm AF} = \frac{\sum_{g=1}^{G} l_{\mathcal{X}_g}}{G}.$$
 (20)

Although this AF method is simple, there may be a large offgrid gap between the obtained equivalent grid point and the real-life channel response.

The AF method considers the true channel responses to be located at the center of the cluster. However, this assumption is usually invalid. Generally, the larger the mean value of a grid point, the closer it is to the real-life channel response. To achieve a more accurate equivalent grid point, a weighted fusion (WF) strategy can be employed. The weight β_g of each grid point in the cluster can be determined by the mean, i.e,

$$\beta_g = \frac{|\mu_g|}{\sum_{g=1}^G |\mu_g|},\tag{21}$$

where $1 \leqslant g \leqslant G$. Therefore, the position of the equivalent grid point can be calculated as

$$k_{\rm WF} = \sum_{g=1}^{G} \beta_g k_{\chi_g}, \tag{22}$$

$$l_{\rm WF} = \sum\nolimits_{g=1}^{G} \beta_g l_{\chi_g}. \tag{23}$$

After fusion, the hyperparameter α corresponding to the equivalent grid point can be calculated as

$$\alpha_{\rm WF} = \sum_{g=1}^{G} \alpha_g. \tag{24}$$

The equivalent grid point (k_{AF}, l_{AF}) or (k_{WF}, l_{WF}) will replace the grid point cluster $\{\mathcal{X}_1, \cdots, \mathcal{X}_G\}$. In the following discussion, these two methods are referred to as GE-CAF and GE-CWF, respectively.

TABLE I: Simulation parameters

Parameter	Value
DD grid size	N = M = 32
Carrier frequency	fc = 4 GHz
Subcarrier spacing	$\Delta f = 15 \text{ kHz}$
Number of channel paths	P = 5
The channel coefficient	$h_i \sim \mathcal{CN}\left(0, \frac{\exp(-0.1l_{\tau_i})}{\sum_i \exp(-0.1l_{\tau_i})}\right)$
Maximum delay	$\tau_{\rm max} = 8.3 \times 10^{-6} \text{ s}$
Maximum relative velocity	500 km/h

D. Adjustment Process

For the GE-CF scheme, after the fusion process, a non-uniform DD grid with better CE performance will be obtained. However, the off-grid gap of the current DD grid cannot be ignored. This is because the CE performance may be affected by the fractional channel. Therefore, adjustment process is required to further reduce the approximation errors.

For the grid point (k_i, l_i) with $|\mu(i)| > \varepsilon \sqrt{\lambda^{-1}}$, the adjustment process is given by

$$\begin{cases} k_i \leftarrow k_i + \kappa_i \\ l_i \leftarrow l_i + \iota_i \end{cases}$$
 (25)

When the adjustment process is completed, the off-grid parameters k_i and l_i will be reduced, leading to decreased Taylor approximation errors $o(\kappa_i)$ and $o(\iota_i)$. Since κ_i and ι_i are integrated into the delay and Doppler values of a grid point, $\Phi(S, \kappa, \iota)$ should be recalculated but this incurs a higher complexity. In this case, an adjustment stop criterion is required. The iteration of the adjustment process will stop if $\|[\kappa^{(k)}, \iota^{(k)}]\| < \delta_a$ or the maximum number of iterations K_a for the adjustment process is reached, where δ_a is a tolerance.

IV. COMPLEXITY ANALYSIS AND SIMULATION RESULTS

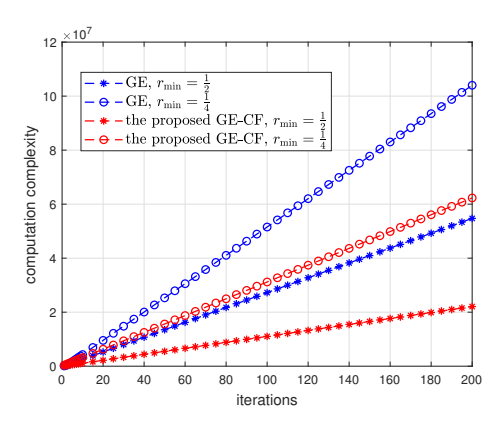


Fig. 2: Accumulated computational complexity comparison.

The proposed GE-CF scheme is compared with GE [10]. Table I presents the simulation parameters. The pilot pattern and guard interval in [7] are used. The power of single pilot is 30 dB higher than the average power of data. In GE, $a=b=10^{-4},~\rho=10^{-2},~\delta=10^{-3},~\delta_{\rm a}=10^{-1},~d=r_{\rm min},~K_{\rm f}=5,~K_{\rm a}=50,~K=200.$ If not stated otherwise, the resolution of the uniform grid scheme is $r=r_{\nu}=r_{\tau}=\frac{1}{4}.$ The initial resolution in the GE scheme is 1, and $r_{\rm min}=\frac{1}{2}$ or $\frac{1}{4}.$

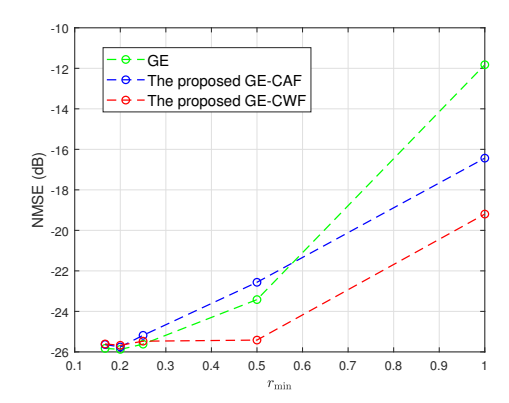


Fig. 3: NMSE under different r_{\min}

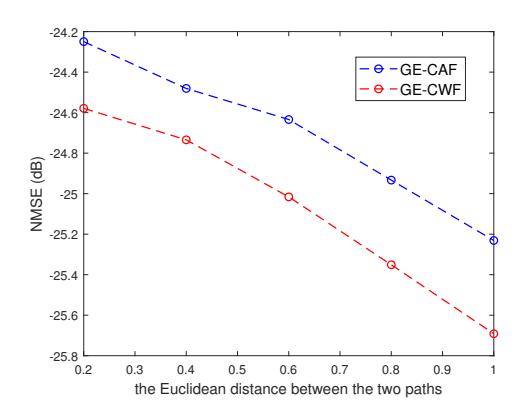


Fig. 4: NMSE versus the Euclidean distance between two paths

The accumulated complexity comparison at different numbers of iterations is shown in Fig. 2. The main complexity of the GE and GE-CF schemes is the same as that of the scheme in [7]. For the GE-CF scheme, the fusion process reduces the number of grid point clusters, resulting in a significant reduction in complexity.

Fig. 3 shows the comparison of NMSE for different $r_{\rm min}$ at SNR = 20 dB. It is found that the NMSE of GE-CAF and GE-CWF is smaller if $r_{\rm min}$ is smaller. In addition, The GE-CWF scheme has the best performance when $r_{\rm min}$ is large.

The NMSE comparison of different inter-path Euclidean distances at SNR = 20 dB and $r_{\rm min}$ = 0.25 is shown in Fig. 4. The larger the Euclidean distance between paths, the smaller the interference between paths and the more accurate the cluster selection, resulting in better CE performance.

The NMSE comparison between different methods is given in Fig. 5. When $r_{\rm min}=0.25$, the NMSE of the proposed GE-CF scheme is similar to that of the GE scheme. When $r_{\rm min}=0.5$, the NMSE of the proposed GE-CWF scheme is significantly better than that of the GE scheme. Considering all simulation results together, the GE-CF scheme achieves a better trade-off between CE performance and computational complexity compared with the GE scheme. In addition, the GE-CWF scheme provides a better trade-off in terms of performance and complexity than the GE-CAF scheme.

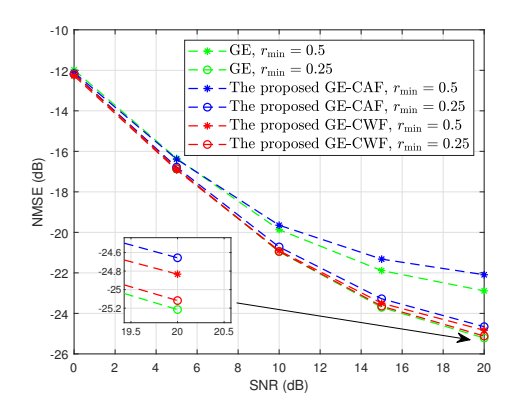


Fig. 5: NMSE comparison

V. CONCLUSIONS

An improved GE-CF method for doubly fractional CE has been proposed in this letter. The proposed GE-CF method consists of four processes, i.e., learning, fission, fusion, and adjustment process. The learning process estimates the channel response at the current grid points, the fission process adds new grid points, the fusion process obtains the equivalent grid point of the grid point cluster, and the adjustment process employs off-grid parameters to adjust the DD grid. Simulation results show that the proposed GE-CF scheme achieves an excellent trade-off between the CE performance and complexity.

REFERENCES

- [1] R. Hadani, S. Rakib, M. Tsatsanis, A. Monk, A. J. Goldsmith, A. F.Molisch, and R. Calderbank, "Orthogonal time frequency space modulation," *IEEE Wireless Communications and Networking Conference (WCNC)*, San Francisco, CA, USA, pp. 1-6, 19-22, March, 2017.
- [2] P. Raviteja, K. T. Phan and Y. Hong, "Embedded pilot-aided channel estimation for OTFS in delay–Doppler channels," *IEEE Trans. Vehicular Technology*, vol. 68, no. 5, pp. 4906-4917, May 2019.
- [3] P. Raviteja, K. T. Phan, Y. Hong and E. Viterbo, "Interference cancellation and iterative detection for orthogonal time frequency space modulation," *IEEE Trans. Wireless Communications*, vol. 17, no. 10, pp. 6501-6515, Oct. 2018.
- [4] W. Shen, L. Dai, J. An, P. Fan, and R. W. Heath, "Channel estimation for orthogonal time frequency space (OTFS) massive MIMO," *IEEE Trans. Signal Process.*, vol. 67, no. 16, pp. 4204-4217, Jul. 2019.
- [5] L. Zhao, W. Gao, and W. Guo, "Sparse bayesian learning of delay-doppler channel for OTFS system," *IEEE Communications Letters*, vol. 24, no. 12, pp. 2766–2769, 2020.
- [6] Z. Yang, L. Xie and C. Zhang, "Off-grid direction of arrival estimation using sparse Bayesian inference," *IEEE Trans. Signal Processing*, vol. 61, no. 1, pp. 38-43, Jan. 2013.
- [7] Z. Wei, W. Yuan, S. Li, J. Yuan and D. W. K. Ng, "Off-grid channel estimation with sparse Bayesian learning for OTFS systems," *IEEE Trans. Wireless Communications*, vol. 21, no. 9, pp. 7407-7426, Sept. 2022.
- [8] Q. Wang, Y. Liang, Z. Zhang, P. Fan, "2D off-grid decomposition and SBL combination for OTFS channel estimation," *IEEE Trans. Wireless Communications*, vol.22, No.5, pp. 3084-3098, May 2023.
- [9] Q. Wang, Z. Zhao, Z. Chen and Z. Nie, "Grid evolution method for DOA estimation," *IEEE Trans. Signal Processing*, vol. 66, no. 9, pp. 2374-2383, May, 2018.
- [10] X. Li, P. Fan, Q. Wang and Z. Liu, "Grid Evolution for Doubly Fractional Channel Estimation in OTFS Systems," *IEEE Trans. Vehicular Technology*, vol. 74, no. 2, pp. 3486-3490, Feb. 2025.
- [11] Y. Shan, F. Wang, Y. Hao, J. Yuan, J. Hua and Y. Xin, "Off-grid channel estimation using grid evolution for OTFS systems," *IEEE Trans. Wireless Communications*, vol. 23, no. 8, pp. 9549-9565, Aug. 2024.